NEUROSCIENCE of Consciousness

Neuroscience of Consciousness, 2025, **2025(1)**, niaf028

DOI: https://doi.org/10.1093/nc/niaf028

Research Article

Longitudinal characterization of electroencephalography features in consciousness recovery following severe traumatic brain injury: a case series study in male patients

Beatrice P. De Koninck[1,2,3,4], Charlotte Maschke[5,4], Marie-Michèle Briand[2,6], Amélie Apinis-Deshaies[2], Daphnee Brazeau[1,2], Rosalie GirardPepin[2,7], Geraldine Martens[2], Virginie Williams[2], Caroline Arbour[2,8], David Williamson[2,9], Catherine Duclos[2,10,11], Francis Bernard[2,7], Stefanie Blain-Moraes[3,4], Louis De Beaumont[2,12,*]

[1]Department of Psychology, Université de Montréal, Montreal, QC, H3C 3J7, Canada
[2]Hôpital du Sacré-Coeur-de-Montréal, CIUSSS du Nord-de-l'Île-de-Montréal Research Center (CRHSCM), Montreal, Montreal, QC, H4J 1C5, Canada
[3]School of Physical and Occupational Therapy, Faculty of Medicine, McGill University, Montreal, QC, H3G 2M1, Canada
[4]Montreal General Hospital, McGill University Health Centre, Montreal, QC, H3H 1V6, Canada
[5]Integrated Program in Neuroscience, McGill University, Montreal, QC, H3A 2B4, Canada
[6]Hôpital du Sacré-Coeur de Montréal, Physical Medicine and Rehabilitation Department, Montreal, QC, H4J 1C5, Canada
[7]Faculty of Medicine, Université de Montréal, Montreal, QC, H3T 1J4, Canada
[8]Faculty of Nursing, Université de Montréal, Montreal, QC, H3S 2N4, Canada
[9]Faculty of Pharmacy, Université de Montréal, Montreal, QC, H3T 1J4, Canada
[10]Department of Anesthesiology and Pain Medicine, Université de Montréal, Montreal, QC, H3T 1J4, Canada
[11]Department of Neurosciences, Université de Montréal, Montreal, QC, H3T 1J4, Canada
[12]Department of Surgery, Université de Montréal, Montreal, QC, H3C 3J7, Canada

*Corresponding author. Hôpital du Sacré-Coeur-de-Montréal, CIUSSS du Nord-de-l'Île-de-Montréal Research Center (CRHSCM), Montreal, QC, Canada. E-mail: louis.debeaumont@umontreal.ca.

Abstract

Crucial clinical decisions in the acute-to-subacute stages of severe traumatic brain injury (sTBI) are mostly based on neurological exams and behavioral assessments. Although electroencephalography (EEG)-derived indices of consciousness show prognostic potential, their effectiveness in tracking individual recovery over time remains unclear. This study characterizes the longitudinal recovery of consciousness following sTBI, tracking EEG spectral power, and aperiodic exponent markers, considering sex, etiology, and age. Four medically stable, non-sedated sTBI patients were recruited 7–26 days post-injury, based on etiology (sTBI), age ($M = 30$ years, $SD = 1.41$ years), lesion severity (diffuse axonal injury). Behavioral responsiveness was assessed daily using the Coma Recovery Scale-Revised (CRS-R), alongside 5-min resting-state EEG for 6 days, with an additional recording a week later. Changes in power spectral distribution and the aperiodic component were observed over time, even within similar diagnostic categories. The aperiodic component exhibited a similar improvement trajectory to behavioral responsiveness, with a progressive flattening of the EEG slope in two individuals who recovered consciousness. In contrast, individuals whose CRS-R category remained static showed inconsistent fluctuations in the aperiodic component over time. Improvements in CRS-R scores were accompanied by changes in absolute power for theta, alpha, and beta frequency bands. However, the "ABCD" and Maximum Frequency Peak frameworks showed limitations and inconsistencies when compared to behavioral outcomes. This longitudinal within-subject design captured neurophysiological changes along patient-specific recovery trajectories, revealing substantial fluctuations within individual EEG markers, despite controlling for typical confounds like etiology, age, lesion severity, and sex. Combining spectral power and the aperiodic exponent may support the development of more dynamic and reliable markers to track changes in brain activity associated with consciousness recovery, potentially improving diagnostic accuracy, outcome prediction, and therapeutic interventions. Ethical approval for this study has been given by the Research Ethics Board of the CIUSSS du Nord-de-l'Île-de-Montréal (Project ID 2021-2279).

Keywords: EEG; severe traumatic brain injury; disorders of consciousness; acute–subacute care

Introduction

Severe traumatic brain injury (sTBI) involves extensive brain damage resulting from a high-magnitude impact. Patients who survive their injuries often fully emerge from a coma, but a portion of the survivors may transition to a disorder of consciousness (DoC), marked by varying impairments of arousal and/or awareness (Laureys et al. 2004, Gosseries et al. 2014, Edlow, Claassen, et al., 2021a). The temporal progression toward recovery varies between

Received 8 November 2024; **revised** 30 July 2025; **accepted** 31 July 2025

patients, as some may progress through different states of DoC, while others may remain in a particular state for a prolonged period (Teasdale and Jennett 1974, Giacino et al. 2018, Edlow, Claassen, et al., 2021a, Alnagger et al. 2023).

In the acute-to-subacute stages after the insult (e.g. <28 days post injury for acute; Giacino et al. 2018), decisions about treatment and continuation of life-sustaining therapy must be made, relying primarily on the combination of neurological examinations and behavioral assessments (Giacino et al. 2014, Gosseries et al. 2014, Edlow et al. 2017, Cassol et al. 2018, Fins 2019). Currently, the most widely used tool in research for detecting signs of awareness at the bedside in patients with DoC is the Coma Recovery Scale-Revised (CRS-R) (Giacino et al. 2004). However, this tool relies on behavioral responses, which can be subject to confounding factors (e.g. concomitant medical conditions compromising intentional behavior, discomfort, and fatigue) that hinder the detection of the presence of awareness (Schiff 2015, Jöhr et al. 2020, Claassen et al. 2023). Indeed, it is now widely understood that lack of behavioral responsiveness does not equate to lack of awareness, and tools that rely only on behavioral responses could miss covert awareness in some patients (Giacino et al. 2009, Stender et al. 2014, Edlow et al. 2017, Bodien et al. 2024). In addition, the CRS-R requires advanced training and a substantial amount of time to administer and interpret, thus necessitating resources that are limited in most hospitals.

Tracking neurophysiological and behavioral markers of awareness over time helps to trace the high frequency of fluctuations in global states of consciousness in this population (Giacino et al. 2009, Wannez et al. 2017, Seth and Bayne 2022). Emerging insights have been derived from indices of consciousness captured by electroencephalography (EEG), such as the power spectral density (PSD), complexity and criticality, functional connectivity, and the aperiodic component (Lehembre et al. 2012, King et al. 2013, Sitt et al. 2014, Colombo et al. 2019, 2023, Wutzl et al. 2021, Frohlich et al. 2022, Toker et al. 2022, Walter and Hinterberger 2022, Liu et al. 2023, Maschke et al. 2023). EEG is a valuable technique at bedside, is affordable, and easily implementable (Jordan 1995). Identifying EEG markers and mechanisms underlying recovery of consciousness after brain injury could not only expand the currently limited therapeutic avenues, but also contribute to advancing diagnostic accuracy and early prediction of outcomes (Gosseries et al. 2014, Giacino et al. 2018, Edlow et al., 2021).

In the past, most research on EEG markers of consciousness focused primarily on the reduction or loss of oscillatory power, with a specific emphasis on the alpha bandwidth (Chennu et al. 2014, 2017, Piarulli et al. 2016, Maschke et al. 2024). In recent years, there has been a shift in focus to the aperiodic component of EEG (i.e. exponential decay of power over frequency), which has been associated with states of consciousness measured behaviorally (Colombo et al. 2019, 2023, Lendner et al. 2020, Maschke et al. 2023, 2024). The aperiodic slope reflects the distribution of power across frequency bands, and the current theory suggests it would indicate the brain's excitatory/inhibitory balance, with reduced consciousness linked to a steeper slope, suggesting increased inhibition and suppressed neural activity propagation (Gao et al. 2017, Colombo et al. 2019, Lendner et al. 2020). Additionally, alternate metrics have been proposed, such as spatial ratios (Colombo et al. 2023), and the location of the maximal peak (Drążyk et al. 2024) to provide greater sensitivity for measuring levels of consciousness.

In addition to the specific description of periodic and aperiodic components of the human EEG, there have been recent proposals for more holistic descriptions. The "ABCD" model was suggested by Forgacs et al. (2017) for neurological recovery assessment in DoC patients who had suffered severe anoxic brain injury. This model describes different EEG spectral profiles to categorize acute patients based on their corticothalamic integrity (Forgacs et al. 2017). Curley et al. (2022) applied the "ABCD" framework in sTBI patients and highlighted its ability to capture and monitor fluctuations of consciousness and to detect improvements in thalamocortical integrity. Building on this work, Drążyk et al. (2024) introduced an alternate model of classifying prolonged DoC based on aperiodic and periodic EEG activity. Type I patients are characterized by low cortical excitability and significant thalamocortical dysfunction and have an EEG spectral profile dominated by the aperiodic component (Rosanova et al. 2012, Drążyk et al. 2024). This category aligns with profile A in the "ABCD" framework (Schiff 2016) and corresponds to a behavioral diagnosis of unresponsive wakefulness syndrome (UWS) (Schiff 2023, Drążyk et al. 2024). Type II patients are characterized by a single oscillatory peak in the theta-alpha range (4–14 Hz), the frequency of which correlates with the patient's CRS-R score and MCS diagnosis. Type III patients have multiple oscillatory peaks (1–14 Hz), which may result from underlying cortical or sub-cortical lesions producing slow rhythms mixed with a Type II profile (Drążyk et al. 2024), thereby complicating alignment with CRS-R diagnostic categories. Using both frameworks provides complementary insights, as the ABCD model offers a classification of thalamocortical integrity, while the maximal peak frequency (MPF) approach is suited to capture subtle, longitudinal shifts in dominant oscillatory peaks (Forgacs et al. 2017, Curley et al. 2022, Drążyk et al. 2024). Taken together, it can provide a diagnostic reference point, and a sensitive measure of neurophysiological changes toward recovery.

While promising, such EEG profiles have yet to be applied to track the recovery trajectory of patients in an acute DoC across etiologies. To date, EEG in DoC patients has been primarily compared on a group-level to healthy adults or across diagnostic categories (Sitt et al. 2014, Engemann et al. 2018, Colombo et al. 2019, 2023). This approach does not readily translate to EEG markers that reliably track within-subject changes as effects observed at the group level are subject to considerable between-subject variability due to factors such as brain lesion, age, sex, and phenotypes. Longitudinal designs that track time-varying EEG markers within the same individual are a crucial first step toward unbiased, personalized monitoring tools for DoC. Curley et al. (2022) highlighted the need for repeated assessments and caution regarding DoC patients with sTBI, as they can be prone to frequent shifts in levels of consciousness within short time periods (2-h windows) (Schnakers et al. 2009, Casali et al. 2013, Gibson et al. 2014, Kondziella et al. 2016, Piarulli et al. 2016, Wannez et al. 2017, Giacino et al. 2018, Demertzi et al. 2019, Curley et al. 2022). By treating each patient as their own control and applying repeated-measures analyses, we increase sensitivity to detect meaningful neurophysiological changes (Sitt et al. 2014, Engemann et al. 2018, Colombo et al. 2019, Donoghue et al. 2020, Lendner et al. 2020), while minimizing confounds related to between-subject heterogeneity. Extending the work of Curley et al. (2022), this study characterizes the longitudinal progression through different states of consciousness in four acute-to-subacute patients who suffered a sTBI. This longitudinal paradigm uses resting-state EEG recording and behavioral measurements to investigate the robustness of candidate EEG markers in indexing changes in consciousness levels within individuals. This case series is a retrospective analysis of a subsample selected from a larger longitudinal cohort, with strict control over etiology, age, sex, and lesion severity to reduce between-subject variability. Our aim is to evaluate these candidate markers based on their robustness,

clinical relevance, and applicability to the acute-to-subacute DoC context. The identification of EEG markers of consciousness that meet these criteria will improve specificity in DoC research, the clinical decision-making processes, and therapeutic interventions for patients with DoC.

Materials and methods

Ethics and study design

This study was approved by the Research Ethics Board of the CIUSSS du Nord-de-l'Île-de-Montréal (Project ID 2021–2279). As participants could not provide informed consent, their legal representatives were informed about the study and provided consent following principles of the Declaration of Helsinki.

Participants

Four medically stable brain-injured, non-sedated patients recruited from the intensive care unit (ICU) of the Hôpital du Sacré-Coeur-de-Montréal, a university-affiliated Level 1 Trauma Center in Montreal, Quebec, Canada. These patients were retrospectively selected from a larger pilot intervention study of 11 patients with severe acquired brain injury (De Koninck et al. 2024). The full cohort included both male and female participants (three women), but for this retrospective case series study selection was based on convergence in key clinical characteristics to reduce between-subject variability and enable a more homogeneous analysis of longitudinal EEG markers. Due to significant differences in age (up to ∼30 years), etiology, and lesion profiles, the female participants did not meet these criteria for inclusion in this focused sub-analysis.

All four participants were enrolled during the acute stage of DoC (<28 days post injury). For three participants, the protocol extended into the subacute stage (i.e. period in which gradual improvements in arousal and awareness may occur either in hospital or rehabilitation facilities) (Giacino et al. 2014, 2018). To control for high between-subject variability, we selected patients based on a similar severe TBI profile—with an initial Glasgow Coma Scale ≤8 and magnetic resonance imaging (MRI)-confirmed Stage 3 diffuse axonal injury (DAI)—to minimize structural heterogeneity, ensuring that observed longitudinal EEG changes primarily reflect recovery of consciousness. Patients were also selected based on sex (male), age ($M = 30$ years, $SD = 1.41$ years), and their trajectory across levels of consciousness (see Table 1). Two patients had a trajectory of improvement in their level of consciousness, beginning from UWS and ending at Emergence from minimally conscious state (eMCS). Two patients had a static trajectory, fluctuating between UWS and MCS− across the entire study.

Inclusion criteria

To be eligible for the study, participants had to: (1) be adults aged 18 or older; (2) have a diagnosis of sTBI and be treated at the ICU; (3) have a confirmed diagnosis of a DoC based on two consecutive CRS-R assessments after sedation withdrawal (if applicable); (4) be clinically stable.

Exclusion criteria

Patients were excluded from the study if they had severe medical comorbidities/complications, such as stroke and status epilepticus; pre-existing severe neurological conditions/disorders involving cognitive deficits such as neurodegenerative diseases (e.g. Amyotrophic lateral sclerosis, dementia, Parkinson's), hereditary conditions (e.g. Huntington's Chorea); central nervous system disorders; constant and intense agitation preventing proper application of the EEG equipment; invasive neurological monitoring (intracranial pressure and/or brain tissue oxygenation); aneurysm clip(s); subdural brain electrodes; implantable neurostimulator; or craniotomy without cranioplasty.

Screening, recruitment, and activation

Participants were selected according to the predefined screening criteria. As part of clinical care, participants were sedated before the start of the study, and testing procedures did not begin until at least 24 h following the cessation of continuous sedation. The precise timing of initial data acquisition was then planned based on two factors: the context-sensitive half-life of the administered sedative agents and the cumulative dose received by each participant (see Table 2 for the complete list of agents). Additional agents with central nervous system effects administered as part of medical care were documented (see Table 2) to validate the robustness of EEG indices in the presence of a patient's usual pharmacological regimen.

Protocol

Five-minute high-density resting-state EEG recordings were conducted daily at 10–10:15 a.m. for six consecutive days (Sessions 1–6), with one additional recording a week later (Session 7), with minor timing variations due to clinical factors (i.e. clinical monitoring, or longer CRS-R assessments). An arousal protocol was performed prior to each session to maximize wakefulness, and sleepiness levels, and vigilance scores were systematically monitored and documented, but sessions were not interrupted in case of a vigilance drop.

Demographic and clinical characteristics

The following information was documented for each participant: age, sex, mechanism of injury, Glasgow Coma Scale (GCS) at initial admission, computed tomography (CT) scan, and/or MRI findings including the level of diffuse axonal injuries according to the radiological stage of Gentry (Gentry 1994) (e.g. clinical reports), along with an injury summary (see Table 1) and the list of sedatives and other molecules administered (see Table 2).

Behavioral measurements of consciousness

Coma Recovery Scale-Revised

The CRS-R assessments were administered at the beginning of each session, immediately prior to each resting-state EEG recording. The CRS-R is a standardized and validated tool for assessing patients with DoC (Giacino et al. 2004, Gosseries et al. 2014). It identifies three states: coma (absence of arousal and awareness), UWS (presence of arousal without behavioral signs of awareness), and minimally conscious state (MCS—presence of arousal and fluctuant but reproducible signs of awareness) (Giacino et al. 2004). MCS is divided into two subcategories based on the absence (MCS−) or presence (MCS+) of residual language function (Giacino et al. 2002, Bruno et al. 2011, Thibaut et al. 2020). eMCS is identified by either reliable functional communication or object use (Giacino et al. 2004). The CRS-R comprises six subscales designed to measure hearing, receptive and expressive language, communication skills, visual perception, motor functions, and arousal (Giacino et al. 2004, AbilityLab 2020). The subscales are hierarchical, with low scores associated with reflexive behaviors and high scores reflecting behaviors resulting from cognitive mediation (AbilityLab. 2020). These scores range from a minimum of 0 to a maximum of 23. Scoring is standardized according to criteria of the presence or absence of clearly discernible, defined

Table 1. Demographic information for all four participants (M: Male; sTBI: severe traumatic brain injury; MVA: motor-vehicle accident) and CRS-R assessment outcomes for each participant across days

Demographic information					CRS-R scores									
Cases	Sex	Age	Etiology	Event	Timepoint	Time since injury (days)	Auditory	Visual	Motor	Oromotor/ verbal	Communication	Arousal	Total score	Category
1	M	29	sTBI	Luge accident	Session 1	26	3	4	0	1	0	2	10	MCS+
					Session 2	27	3	1	2	0	0	1	7	MCS+
					Session 3	28	3	4	5	1	0	2	15	MCS+
					Session 4	29	4	5	5	1	1	2	18	MCS+
					Session 5	30	2	4	5	2	0	2	15	MCS−
					Session 6	31	4	4	5	2	0	2	17	MCS+
					Session 7	37	3	5	6	3	1	3	21	eMCS
2	M	30	sTBI	MVA	Session 1	7	1	1	2	1	0	1	6	UWS
					Session 2	8	2	2	2	0	0	2	8	MCS−
					Session 3	9	3	3	5	1	1	1	14	MCS+
					Session 4	10	4	5	6	3	1	3	22	eMCS
					Session 5	11	3	4	6	3	1	3	20	eMCS
					Session 6	12	4	4	6	3	1	3	21	eMCS
					Session 7	18	4	5	6	3	2	3	23	eMCS
3	M	29	sTBI	Ski accident	Session 1	20	2	3	5	1	0	1	12	MCS−
					Session 2	21	2	4	5	1	0	1	13	MCS−
					Session 3	22	3	4	5	0	0	2	14	MCS+
					Session 4	23	3	4	5	1	0	2	15	MCS+
					Session 5	24	4	4	5	1	0	2	16	MCS+
					Session 6	25	3	4	5	1	0	1	14	MCS+
					Session 7	31	4	5	5	3	1	3	21	MCS+
4	M	32	sTBI	MVA	Session 1	26	1	3	1	1	0	1	7	MCS−
					Session 2	27	1	1	2	1	0	2	7	UWS
					Session 3	28	1	3	2	1	0	1	8	MCS−
					Session 4	29	2	3	2	1	0	1	9	MCS−
					Session 5	30	2	3	2	1	0	1	9	MCS−
					Session 6	31	1	3	2	1	0	1	8	MCS−
					Session 7	37	2	3	4	1	0	2	12	MCS−

functional behaviors (AbilityLab 2020). The CRS-R is sensitive enough to distinguish between MCS+ and MCS− (Thibaut et al. 2019, AbilityLab 2020).

High-density electroencephalography

EEG data were recorded using a 128-Channel Geodesic Sensor Net (Magstim-EGI, OR, USA) with sponge-based electrode nets referenced to Cz, at a sampling rate of 1000 Hz. Electrode impedance was kept below 50 kΩ and monitored before each recording. Resting-state brain activity was recorded for 5 min. This high-density setup enabled improved spatial resolution and signal averaging across anatomical regions. However, the further described analyses are compatible with standard lower-density systems commonly used in clinical settings (e.g. 19 channels).

Electroencephalography data analysis

EEG data were pre-processed using MNE software (MNE Developers 2012). Data were bandpass filtered between 1 and 55 Hz, a notch filter was applied at 60 Hz, and the signal was downsampled to 250 Hz. Channels with high levels of non-physiological artifacts were removed manually upon visual inspection. Data were segmented into 10-s windows. Epochs with excessive levels of artifacts (i.e. exceeding a ±2000 μV amplitude threshold) were automatically excluded from further analysis. An additional manual inspection was conducted to remove any remaining epochs containing visible noise by a trained experimenter. Case 1 had high rejection rates in multiple sessions (e.g. 71.4% in ses-01, 70.7% in ses-07), while Case 4 displayed good data quality with minimal rejections across all sessions (0%–28.2%). Cases 2 and 3 showed moderate rejection rates, especially in later sessions (e.g. Case 2: 66.7% in ses-06; Case 3: ∼45% in multiple sessions). These differences in epochs rejection are summarized in Supplementary Table S1.

To further clean the signal from artifacts introduced by muscle and eye movements, a semi-automated independent component analysis pipeline available in the MNE-Python library (Gramfort et al. 2013) was applied. Data were average-referenced and non-brain electrodes were removed for subsequent analyses.

Electroencephalography spectral features

The following EEG features were selected based on their strong evidence as electrophysiological markers of consciousness, their ease of use, practical application, and clear interpretability. The EEG oscillatory power spectrum remains an established and widely used method for assessing brain injured patients with a DoC, due to its simple computation and effectiveness in monitoring brain activity change. Indices derived from PSD analyses such as the spatial power gradient (Colombo et al. 2023), maximum peak frequency (MFP) (Drążyk et al. 2024), and the ABCD framework (Schiff 2016) have been introduced as reliable and visually interpretable markers for tracking fluctuations in consciousness. On the other hand, the aperiodic component

Table 2. List of pharmacological agents administered before and during the study protocol

Case number	Sedation prior to protocol	Drug class (prior)	Mechanism of action	Last administration (pre-protocol)	Administered agents (during protocol)	Drug class (during)	Mechanism of action	Additional information
1	Midazolam	Benzodiazepine	GABA-A receptor agonist	11 days	Amantadine	Antiviral and Anti-Parkinsonian Agent	NMDA receptor antagonist Dopamine reuptake inhibitor	Administration initiated more than 48 h before assessment
					Clonidine	Antihypertensive	a2-Adrenergic receptor agonist	
					Propanolol	Beta blocker	β1 and β2 Adrenergic receptors antagonist	
	Dexmedeto-midine	Sedative and analgesic	a2-Adrenergic receptor agonist	10 days	Hydromorphone	Opioid analgesic	μ-Opioid receptor agonist	Assessments timed according to the half-life of the drug's duration of action
	Fentanyl	Opioid analgesic	μ-Opioid receptor agonist	10 days	Acetaminophen	Analgesic and antipyretic	Non-opioid analgesic	
					Quetiapine	Atypical antipsychotic	Dopamine D2 receptor antagonist Serotonin 5-HT2A receptor antagonist	
2	Fentanyl	Opioid analgesic	μ-Opioid receptor agonist	4 days	Hydromorphone	Opioid analgesic	μ-Opioid receptor agonist	Assessments timed according to the half-life of the drug's duration of action
	Propofol	Sedative and general anesthetic	Positive modulation of GABA-A receptors	4 days	Clonidine	Antihypertensive	a2-Adrenergic receptor agonist	
	Midazolam	Benzodiazepine	GABA-A receptor agonist	3 days				
3	Propofol	Sedative and General Anesthetic	Positive modulation of GABA-A receptors	8 days* only for hospital transfer	Hydromorphone	Opioid analgesic	μ-Opioid receptor agonist	Assessments timed according to the half-life of the drug's duration of action
					Propanolol	Beta blocker	β1 and β2 Adrenergic receptors antagonist	
					Acetaminophen	Analgesic and antipyretic	Non-opioid analgesic	
					Amantadine	Antiviral and dopaminergic agent	NMDA receptor antagonist Dopamine reuptake inhibitor	Administration initiated more than 48 h before assessment
4	Dexmedeto-midine	Sedative and analgesic	a2-Adrenergic receptor agonist	8 days	Clonidine	Antihypertensive	a2-Adrenergic receptor agonist	
					Propanolol	Beta blocker	β1 and β2 Adrenergic receptors antagonist	
					Acetaminophen	Analgesic and antipyretic	Non-opioid analgesic	

shows great potential as a marker of consciousness by capturing additional information about the cortical excitability, independently of oscillatory activity (Lendner et al. 2020, Donoghue et al. 2021, Maschke et al. 2023).

The PSD

The PSD was calculated for each channel across the entire recording session using Welch's method (MNE-Python; Gramfort et al. 2013), with a frequency range of 1–45 Hz (i.e. minimal and maximal frequencies of interest), 2-s window length, 50% overlap between segments, and a fast Fourier transform window length of 500 samples (with 250-sample overlap). Frequency bands were defined as: delta [1–4 Hz], theta [4–8 Hz], alpha [8–13 Hz], beta [13–30 Hz], and gamma [30–45 Hz].

PSD was also calculated separately, using the same parameters, for each brain region and hemisphere (i.e. frontal, central, parietal, occipital, and temporal; right and left) to preserve regional differences. This approach identifies distinct oscillatory patterns that may be masked by whole-brain averaging. This method was chosen to better classify the MFP and ABCD profiles, as described later.

Absolute power

Absolute power (i.e. total power within a specific frequency band) was computed by taking the $\log_{10}$ of the area under the PSD curve (in $\mu V^2/Hz$) within each frequency band, then averaged across channels.

Spatial gradient

Based on previous work by Colombo et al. (2023) who introduced the posterior–anterior ratio (PAR), we calculated the EEG spatial gradients across different frequency bands. This ratio is defined as the division of the geometric mean of all posterior values of absolute power by the geometric mean of anterior values of absolute power, yielding a numerical value of the distribution of a frequency band across the brain. The line separating the anterior and posterior brain regions is placed transversely from the ears and aligned with Cz on the midline. Electrodes overlapped by this line were excluded from the analysis. Ratio values between 0 and 1 show anterior-dominant activity within the targeted frequency band, whereas ratio values above 1 show posterior-dominant activity.

Aperiodic component

Aperiodic components of the power spectrum, specifically the spectral exponent (i.e. how the power decays across frequencies) and offset (i.e. absolute power level of the background activity) were calculated across time for each channel, then averaged across electrodes using the fixed mode of the "fitting oscillation and one over f (FOOOF)" function (Donoghue et al. 2020). Hyperparameters for the peak detection were chosen according to Gerster et al. (2022) recommendations to prevent overfitting and detecting spurious oscillations. We applied a minimum peak height threshold of 0.1, limited the number of detected peaks per spectrum to a maximum of 3, and restricted the peak widths to a range of 0.5–12 Hz.

Maximum peak frequency

In concordance with Drążyk et al. (2024), we identified the highest peak in the 1–14 Hz range using the "FOOOF" package (Donoghue et al. 2020) fit between 1 and 45 Hz. Following Drążyk et al. (2024), the minimum peak height was set to 0.111 μV, with a maximum detection of four peaks and peak width limits of 2–6 Hz. The maximal peak was defined as the highest amplitude peak with a center frequency between 1 and 14 Hz. If no peak was detected in the 1–14 Hz range, the maximal peak was treated as a missing value. Maximal peak detection was calculated on the PSD averaged across all electrodes within each brain region and hemisphere. This averaging process reduces noise, facilitating the detection of peaks that remain stable across most electrodes within a region. A Gaussian filter with a smoothing parameter of $\sigma = 0.5$ was applied solely for plotting purposes to reduce noise and visually assess the profiles. The classification of the PSD into three types was based on the mode (i.e. the most frequently occurring classification (Types I, II, or III)) within each brain area and hemisphere, followed by calculating the mode (or trend) across all areas for a specific time point. In the event of a tie across regional classifications, the classification associated with the highest level of neural recovery was selected.

ABCD

ABCD profiles were also classified based on the same approach as described for the MPF. In case the mode approach was inconclusive, the most promising approach was used. The most promising approach was based on prioritizing the highest level in the recovery hierarchy (D > C > B > A), in this Case D being the highest level of recovery. ABCD profiles were assessed manually by two independent reviewers. In case of a disagreement, a third-party made the final decision.

Clinical follow-up

To provide additional perspective only, we retrospectively extracted Functional Independence Measure (FIM), Glasgow Outcome Scale-Extended (GOSE), and Disability Rating Scale (DRS) scores at 3, 6, and 12 months from the parent study; trajectories are shown in Supplementary Fig. S10.

Results

Case 1

Case 1 was a 29-year-old male who suffered a sTBI due to a sledding collision against a tree. His GCS score upon arrival at hospital was 3. Concomitant brain imaging—MRI and CT—showed Stage 3 DAI (i.e. within midbrain, pons, splenium, right corona radiata, right lenticular nucleus, and basal ganglia), a subdural hematoma in the right frontal region and contusion in the medial temporal lobe bilaterally, and in the left parahippocampal gyrus. In the acute phase of the brain injury, the patient also developed paroxysmal sympathetic hyperactivity. Additional injuries were: C2 transverse process and left costal fractures, left mandibular laceration, minimal bilateral pneumothorax, and pulmonary contusions. For the pharmacological regimen administered, refer to Table 2.

The study was initiated 26 days post-injury. During the 2-week assessment protocol, the participant transitioned across different CRS-R categories. At baseline, he was categorized as MCS+ based on the ability to perform reproducible movements to command. Although his overall CRS-R scores improved almost daily (from 10 to 21), his condition regressed to the MCS− category in Session 5 despite a stable arousal score of 2, as the best behavioral responses were object localization (reaching) and automatic motor responses. Despite this setback, repeated assessments revealed gradual improvements. By the end of the 2-week period, he displayed qualitative attention and progressed to showing functional object use, placing him in the eMCS category

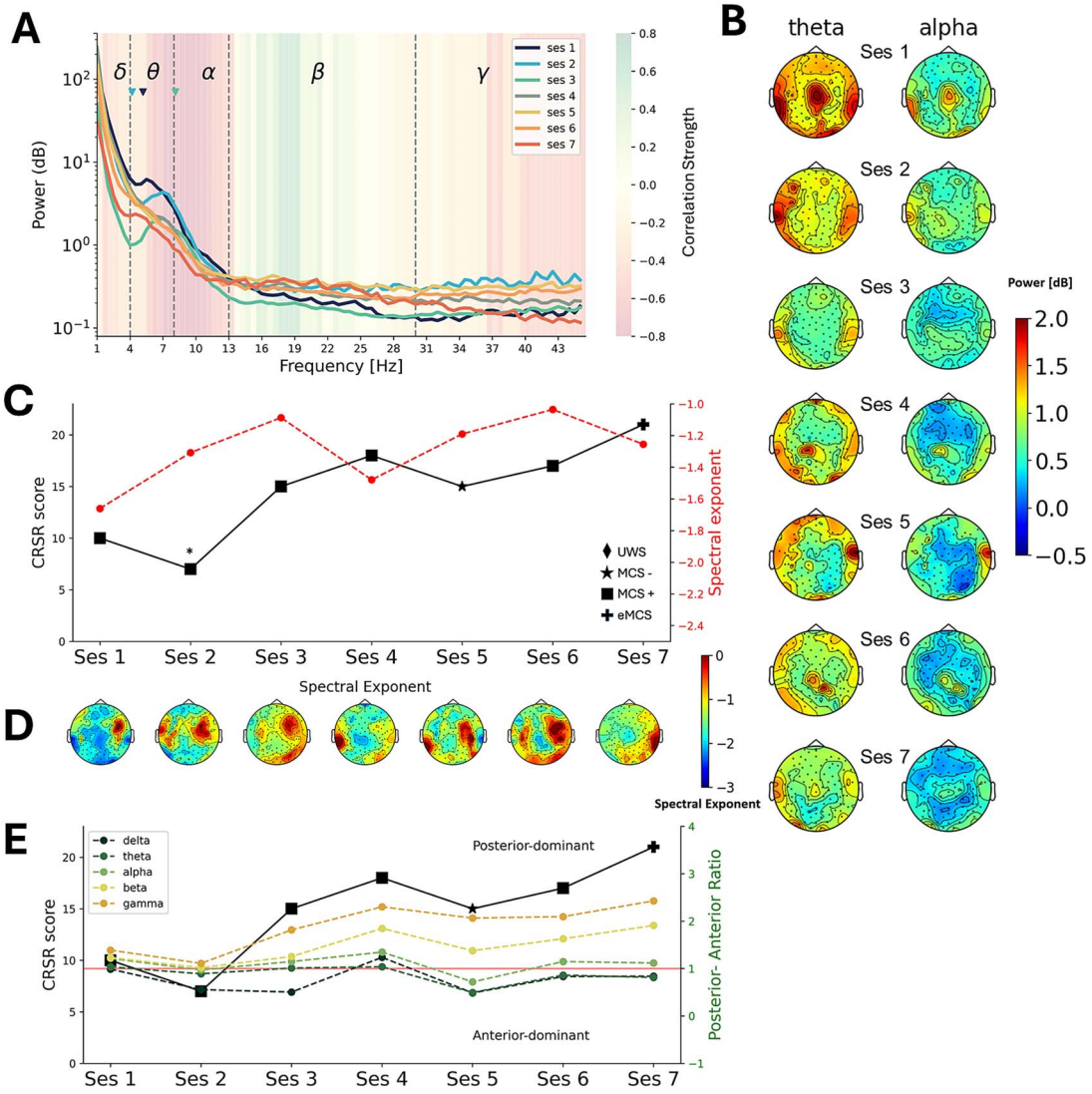

Figure 1. EEG features and progression of behavioral responsiveness over time for all cases. (A) EEG power spectrum density for each consecutive session [1–6] and 1 week after [Session 7], with shaded regions showing Spearman correlations between spectral power and CRS-R scores (negative values indicating higher scores with lower power, positive values indicating higher scores with higher power), and triangles marking the maximal peak frequency in the 1–14 Hz band. (B) Topographic maps of theta and alpha power over all sessions. (C) Temporal development of CRS-R score and spectral exponent over sessions, with marker shapes indicating the participant's diagnosed level of consciousness and asterisks marking sessions in which the patient fell asleep. (D) Topographic maps of the spectral exponent over Sessions 1–7. (E) Posterior–anterior power ratios of all frequency bands over time with the temporal development of CRS-R score.

(confirmed in two consecutive assessments), and reaching an overall CRS-R score of 21 (see Table 1, see Fig. 1C).

At the neurophysiological level, the gradual improvement of behavioral responsiveness was accompanied by an overall decrease in power in lower frequency bands (i.e. delta, theta, alpha) and an increase in power in the beta frequency (Table 1 and Fig. 1A, and Supplementary Fig. S9). PAR analyses revealed an increase in posterior-dominant activity in gamma and beta power across sessions, while the alpha power's slight posterior-dominance remained stable as the CRS-R improved. Theta power progressed from a ratio of 1 (equal distribution) to an anterior-dominant (ratio < 1) activity as the behavioral responsiveness improved. Delta power remained anterior-dominant across sessions (Fig. 1B and E, see Supplementary Fig. S1b for all frequency bands). The peak frequency gradually increased from theta bandwidth (4–8 Hz) to the alpha bandwidth (8–13 Hz) across sessions (Fig. 1A). No clear effect was observed in the gamma frequency band (see Fig. 1A). For a complete overview of MFP according to sessions and cases, refer to Supplementary Table S2.

The global change of the PSD across sessions (i.e. decrease in lower frequency band power, increase in higher frequency band power) was also reflected in an overall flattening of the spectral exponent as the CRS-R scores improved (see Figs 1C and 5A and B, see Supplementary Fig. S1a). Although the behavioral performance captured by the CRS-R assessment was not consistently reflected in the spectral exponent (e.g. a steep exponent in Session 4 despite a higher CRS-R score), an overall progression towards a flatter spectral exponent (i.e. from a minimum of −1.66 on Session 1 to a maximum of −1.04 on Session 6) was observed over sessions. This shift indicates a transition from a predominant low-frequency neural activity to an increased neural activity in the higher frequency bands. The flattening of the spectral exponent was distributed over the whole brain, with the largest change in posterior regions (see Fig. 1D). It is important to note that on

Session 2, the arousal score was 1 during the acquisition despite conducting the arousal protocol, with an episode of sleep during the EEG. However, although behavioral responsiveness was lower, the spectral exponent still reflected a flattening of the slope despite this fluctuation in state.

PSD analyses revealed a single MFP in the 1–14 Hz range. A peak in the theta–alpha bandwidth was observed from Sessions 1 to 3, showing a Type II profile (Drążyk et al. 2024; see Fig. 1A), coherent with the MCS+ behavioral diagnosis for those sessions. However, from Sessions 4 to 7, a transition to a Type I profile (i.e. dominance of the aperiodic component) was observed, which corresponds to a UWS diagnosis (see Fig. 6A). Despite this profile, the patient was assessed behaviorally as MCS−, MCS+ up to eMCS at the seventh session, diverging from the framework. The "ABCD" framework revealed the same pattern sequence. The participant's EEG profile evolved from Type "B" (theta peak; 4–8 Hz) from Sessions 1 to 3, to a type "A" (delta peak; <4 Hz) for Sessions 4 to 7 (see Fig. 6B and Supplementary Fig. S5 for all PSD plots used to classify, see Supplementary Fig. S9 for clusters of electrodes used).

To provide clinical context, Case 1's functional scores progressed from GOSE 4/DRS 10/FIM 70 at 3 months, to GOSE 5/DRS 6/FIM 95 at 6 months, and to GOSE 6/DRS 3/FIM 115 at 12 months (see Supplementary Fig. S10).

Case 2

Case 2 was a 33-old male who suffered a sTBI in a motor-vehicle accident. His GCS score upon arrival at hospital was 7. Brain imaging assessments reported Stage 3 DAI (i.e. in the midbrain-pons junction, the corpus callosum especially in the splenium, cerebellum hemispheres bilaterally, cortical–subcortical junction especially in the frontal lobe bilaterally, but more on the left), possible micro-ischemia at different localizations including the centrum semioval bilaterally, the left sub-insula, para-atrial, central portion of the splenium of the corpus callosum. In addition, subarachnoid hemorrhage, bi-frontal subdural hematoma and left tentorial were observed. Additional injuries included multiple rib fractures bilaterally including the first left rib, left tibia, and fibula fractures, right scapula fracture, vertebral corpus fracture of the third and fourth dorsal vertebrae, fracture of the transversal process of the first and second lumbar vertebrae, bilateral pneumothorax, pneumomediastinum, right hemothorax, right adrenal hemorrhage, and heart and liver contusions. For the pharmacological regimen administered, refer to Table 2.

The study was initiated 7 days post-injury. During the 2-week assessment period, the participant showed consistent improvement in responsiveness resulting in progressions across all categories of the CRS-R from an initial score of 6 to 23 on the last assessment. The participant was categorized as UWS, on Day 1, and progressed to MCS− on Day 2 with the demonstration of fixation (i.e. eyes change from initial fixation point and refixate on the new target location for more than 2 s). On Day 3, he reached MCS+ with reproducible movement to command. From Day 4 onward, the participant showed functional object use with sustained attention, which was confirmed as an eMCS state upon two consecutive assessments (see Table 1 and Fig. 2C).

The participant's improvement in behavioral responsiveness was accompanied by an overall reduction of power in lower frequency bands (i.e. delta, theta, and alpha) and an increase in higher frequency band power (i.e. beta and gamma) (see Table 1 and Fig. 2A, and Supplementary Fig. S9). Theta activity remained anterior-dominant and alpha power remained posterior-dominant across all sessions, whereas delta, beta and gamma remained static with a slight anterior dominance as the participant's level of consciousness improved (Fig. 2B and E, see Supplementary Fig. S2b for all frequency bands).

The global change of the spectral power distribution across sessions (i.e. decrease in lower frequency band power and increase in higher frequency band power) was also captured by an overall flattening of the spectral exponent as CRS-R scores improved (see Figs 2C, and 5A and B, see Supplementary Fig. S2a). For this participant, the behavioral performance progression captured by the CRS-R assessments was consistently reflected in the spectral exponent results, with flatter exponents reflecting higher CRS-R scores (i.e. from a minimum of −2.4 on Session 1 to a maximum of −1.6 on Session 6). The flattening of the spectral exponent was present across the whole brain (see Fig. 2D).

PSD analyses revealed fluctuations of profiles across sessions, alternating between a single MFP in the 1–14 Hz range, indicative of a Type II profile, and the presence of peaks in both theta to alpha bandwidths (see Fig. 6A), corresponding to a Type III profile (Drążyk et al. 2024). Behaviorally, this participant progressed from being assessed as UWS to eMCS over time. According to the "ABCD" framework, the participant's EEG profile evolved from Type "B" (theta peak; 4–8 Hz) at Session 1, to a "non-ABCD" profile from Sessions 2 to 6, with the presence of peaks in theta and alpha bands but no peak in the beta band. By Session 7, the profile reverted to Type "B" (see Fig. 6B, Supplementary Fig. S6 for all PSD plots used to classify).

To provide clinical context, scores moved from GOSE 4/DRS 7/FIM 60 at 3 months, to GOSE4/DRS 7/FIM 70 at 6 months, and to GOSE 4/DRS 5/FIM 80 at 12 months (see Supplementary Fig. S10).

Case 3

Case 3 was a 29-year-old male who suffered a sTBI in a downhill ski accident. His GCS score upon arrival at the hospital was 4, showing decortication. Brain imaging assessment confirmed Stage 3 DAI (i.e. within the brainstem but minimally, bilateral cerebral peduncles, the splenium of the right corpus callosum, the left basal ganglia especially in the left internal capsula, and multiple hemorrhagic foci—left more than right temporal lobes, right mid-frontal lobe, the base of the right frontal lobe). In addition, diffuse subarachnoid hemorrhage to middle frontal, left temporal and biparietal brain regions and subdural hematoma to the cerebellar tent, and intra-ventricular hemorrhages. No additional injury was identified. For the pharmacological regimen administered, refer to Table 2.

The study was initiated 20 days post-injury. Across all sessions, the participant improved by one diagnostic category according to serial CRS-R assessments. At the initial session, the participant was diagnosed to be in MCS− (CRS-R score of 12 and arousal level at eye opening with stimulation) with automatic motor responses. On Session 3, the participant progressed to MCS+ and reached a maximal CRS-R score of 21 on the last session of the study protocol [Session 7] (i.e. 2 weeks after the baseline recording) with sustained attention, consistent movement to commands, object recognition, intelligible verbalization, and non-functional, intentional communication (see Table 1, see Fig. 3C).

Across all sessions, power in the alpha frequency band was posterior-dominant, with the ratio increasing on the date with the best behavioral score of consciousness. Theta power shifted from an equal distribution toward posterior dominant activity across sessions. Delta, beta, and gamma power displayed an equal topographic distribution until the last session, when they became posterior-dominant and the highest CRS-R score was reached (Fig. 3B and E, see Supplementary Fig. S3b for all frequency bands).

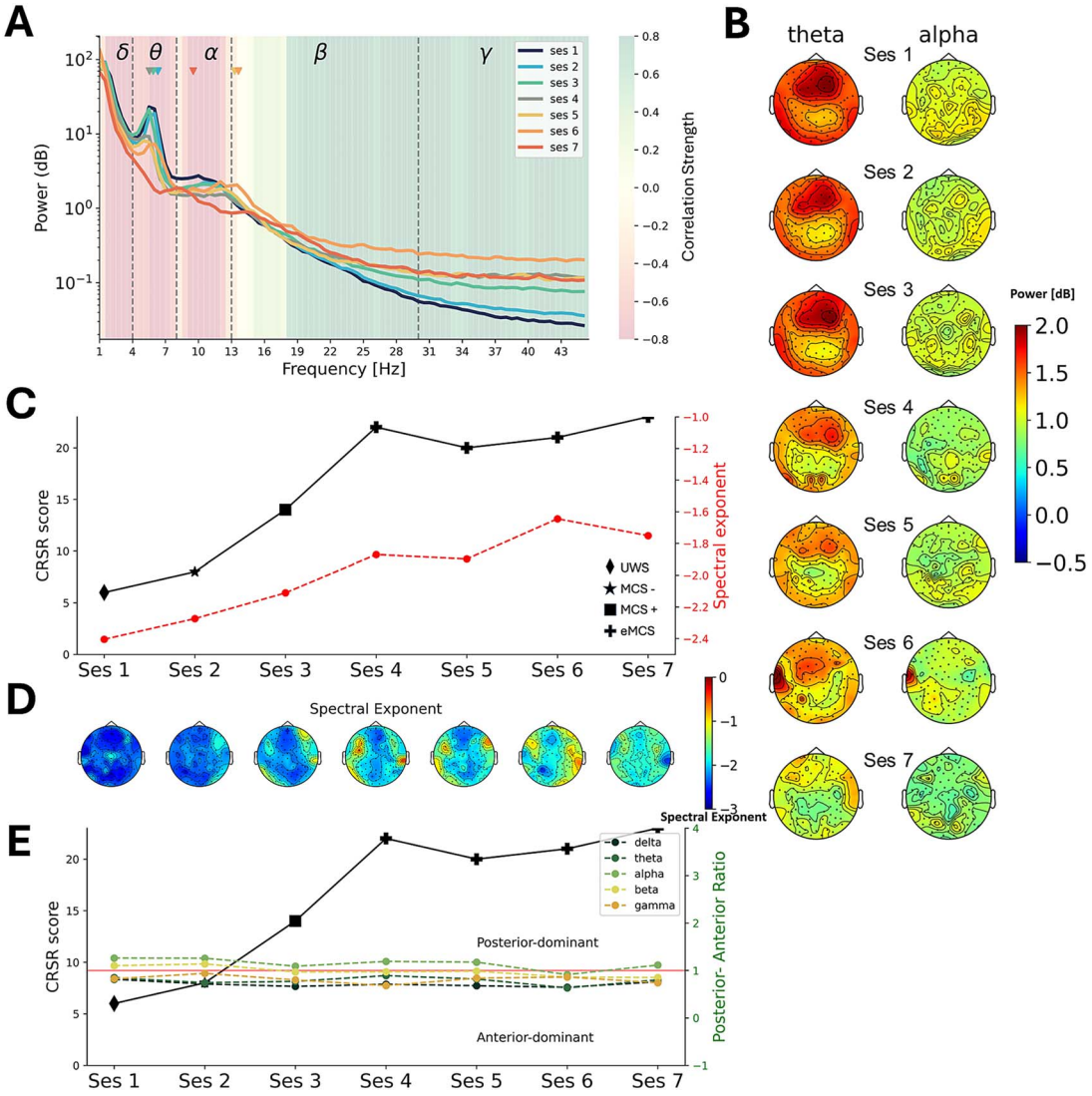

Figure 2. EEG features and progression of behavioral responsiveness over time for all cases. (A) EEG power spectrum density for each consecutive session [1–6] and 1 week after [Session 7], with shaded regions showing Spearman correlations between spectral power and CRS-R scores (negative values indicating higher scores with lower power, positive values indicating higher scores with higher power), and triangles marking the maximal peak frequency in the 1–14 Hz band. (B) Topographic maps of theta and alpha power over all sessions. (C) Temporal development of CRS-R score and spectral exponent over sessions, with marker shapes indicating the participant's diagnosed level of consciousness and asterisks marking sessions in which the patient fell asleep. (D) Topographic maps of the spectral exponent over Sessions 1–7. (E) Posterior–anterior power ratios of all frequency bands over time with the temporal development of CRS-R score.

Contrary to the previous cases, the behavioral improvements reflected by the gradual increase in scores within the MCS+ category were not reflected by the spectral exponent (Figs. 3C and 5A and B, see Supplementary Fig. S3a). Instead, the spectral exponent was characterized by high variability and fluctuation over time, with values ranging from −1.0 in Session 1 to −1.6 in Session 7. Only one sleep episode was observed during Session 6 EEG recording, which corresponded to a steepening of the spectral exponent and concurrent decreases in theta and alpha power. Despite this episode, no alignment between the CRS-R score and the spectral exponent was observed across sessions (see Table 1 and Fig. 3C). Contrary to a consistent slow increase of CRS-R, Sessions 1, 3, and 5 were characterized by a sudden strong flattening of the spectral exponent which was most strongly expressed over anterior brain regions (see Fig. 3D).

Regarding the MPF classification (Drążyk et al. 2024), PSD analyses displayed fluctuating profiles between a Type II with a single peak in the 1–14 Hz range for most sessions and a Type I profile for Sessions 3 and 5 (see Fig. 6A), both sessions associated with flatter spectral exponent (see Fig. 3C). According to the "ABCD" framework, Type "B" profile was observed for almost all sessions coherent with the MFP classification (see Fig. 6B, Supplementary Fig. S7 for all PSD plots used to classify).

To provide clinical context, scores progressed from GOSE 4/DRS 5/FIM 80 at 3 months, to GOSE 5/DRS 3/FIM 95 at 6 months, and to GOSE 6/DRS 1/FIM 115 at 12 months (see Supplementary Fig. S10).

Case 4

Case 4 was a 32-year-old male who suffered a sTBI in a high-speed all-terrain vehicle accident. He was found unconscious, with extensive facial trauma. His initial GCS score was 3. Brain imaging assessments reported Stage 3 DAI (i.e. within the midbrain specifically at the left cerebral peduncle, at the cortical–subcortical junction bilaterally, at the left caudal nucleus, at the genu and splenium of the corpus callosum, and the left

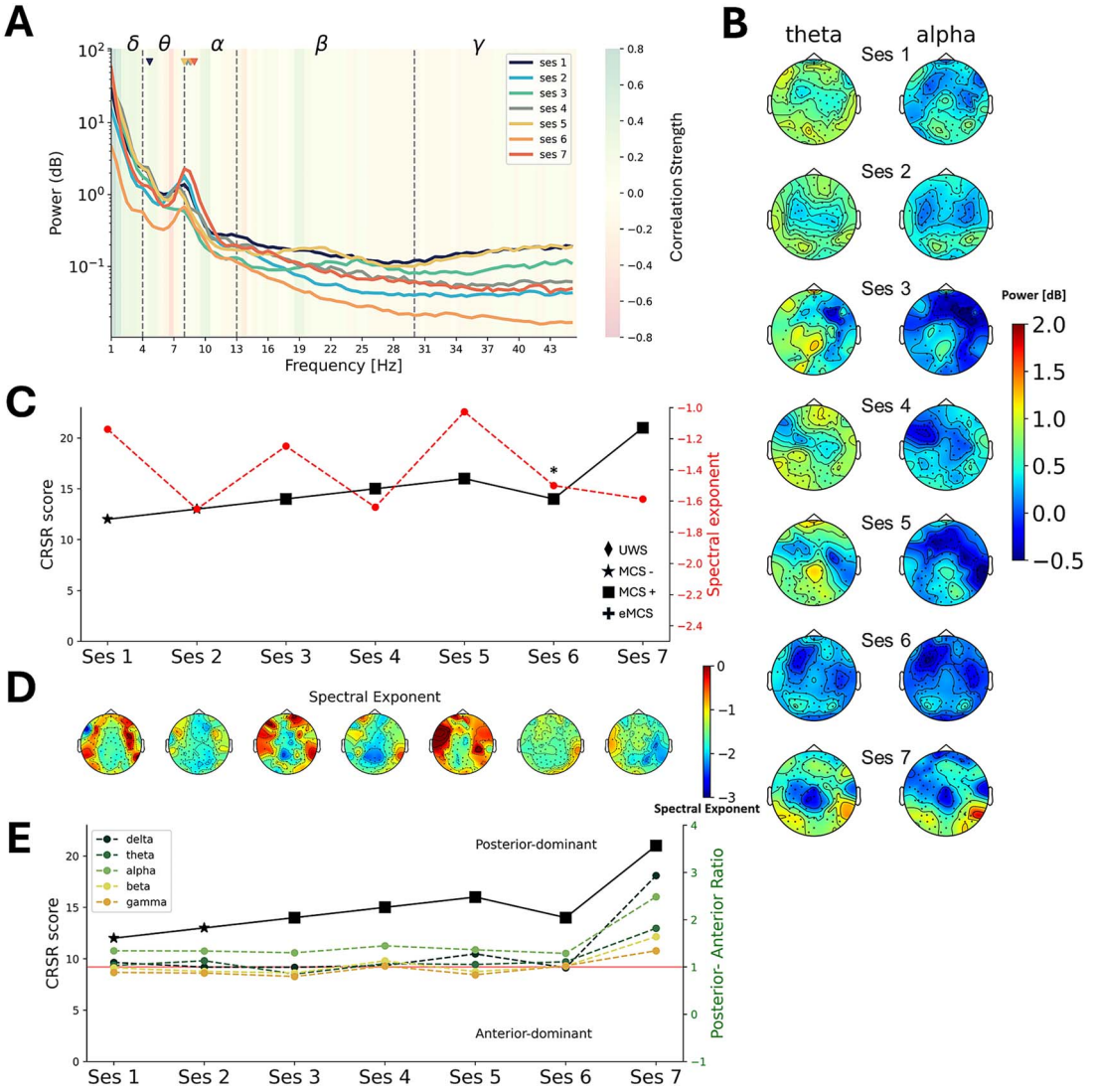

Figure 3. EEG features and progression of behavioral responsiveness over time for all cases. (A) EEG power spectrum density for each consecutive session [1–6] and 1 week after [Session 7], with shaded regions showing Spearman correlations between spectral power and CRS-R scores (negative values indicating higher scores with lower power, positive values indicating higher scores with higher power), and triangles marking the maximal peak frequency in the 1–14 Hz band. (B) Topographic maps of theta and alpha power over all sessions. (C) Temporal development of CRS-R score and spectral exponent over sessions, with marker shapes indicating the participant's diagnosed level of consciousness and asterisks marking sessions in which the patient fell asleep. (D) Topographic maps of the spectral exponent over Sessions 1–7. (E) Posterior–anterior power ratios of all frequency bands over time with the temporal development of CRS-R score.

superior cerebellar peduncle), multiple contusions involving the left temporal uncus, the right opercular temporal and left frontal lobes, minimal subarachnoid hemorrhage, right para facial, bifrontal and left cavernous sinus subdural hematoma, intraventricular hemorrhage, and bilateral occipital intraparenchymal hemorrhage. In the acute phase of the brain injury the patient also developed paroxysmal sympathetic hyperactivity. Additional injuries included nasal bone, right maxillary sinus, fifth cervical vertebrae, and 10th right rib fractures, pancreatic-duodenal junction infiltration, severe acute respiratory distress syndrome, and left carotid aneurysm. For the pharmacological regimen administered, refer to Table 2.

The study was initiated 26 days post-injury. The participant's behavioral responsiveness remained stable over all sessions. At Session 1, the participant was assessed as MCS– based on his visual pursuit, however, he had very weak arousal level. Although his overall CRS-R scores gradually improved from 7 to 12, he remained MCS– on 6 out of 7 assessments. By the end of the sessions, he could reach with eye opening without stimulation, thus showing object localization (see Table 1, see Fig. 4C).

The EEG spectral power broadly increased across sessions, as illustrated in Fig. 4A. The strongest increase was observed in higher frequency bands (i.e. beta and gamma). Lower frequency bands (i.e. delta, theta, alpha) did not exhibit a clear progression pattern over time.

Topographical maps and PAR of power for all frequency bands across sessions displayed a posterior-dominant distribution during initial sessions that shifted to a slight anterior-dominant distribution in the last sessions (Fig. 4B and E, see Supplementary Fig. S4b for all frequency bands).

The spectral exponent exhibited a gradual flattening from a minimum of −2.00 on Session 1 to a maximum of −1.1 on Session 7, despite only minimal changes in behavioral responsiveness (see Figs 4C and 5A and B, see Supplementary Fig. S4a). The flattening

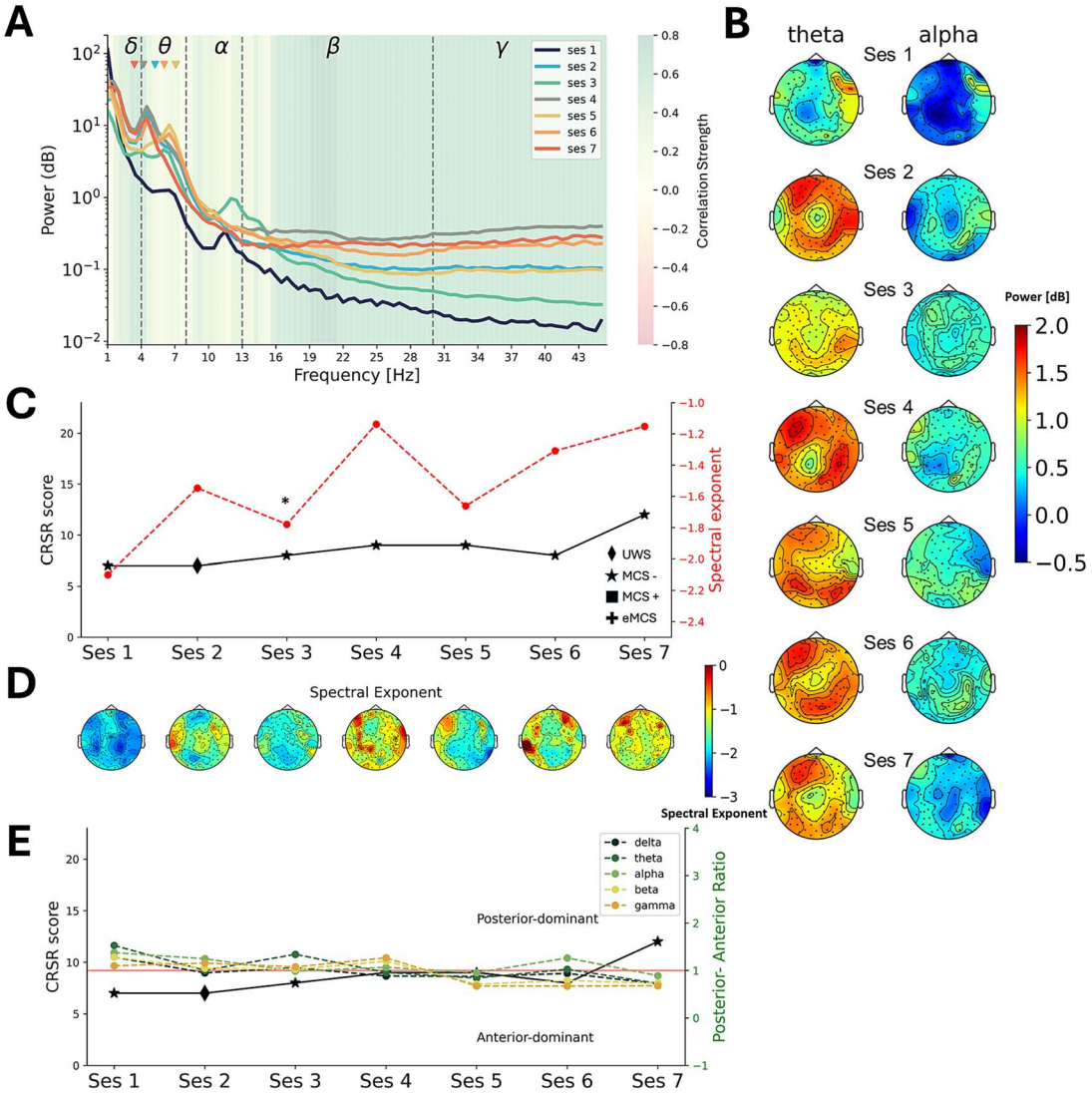

Figure 4. EEG features and progression of behavioral responsiveness over time for all cases. (A) EEG power spectrum density for each consecutive session [1–6] and 1 week after [Session 7], with shaded regions showing Spearman correlations between spectral power and CRS-R scores (negative values indicating higher scores with lower power, positive values indicating higher scores with higher power), and triangles marking the maximal peak frequency in the 1–14 Hz band. (B) Topographic maps of theta and alpha power over all sessions. (C) Temporal development of CRS-R score and spectral exponent over sessions, with marker shapes indicating the participant's diagnosed level of consciousness and asterisks marking sessions in which the patient fell asleep. (D) Topographic maps of the spectral exponent over Sessions 1–7. (E) Posterior–anterior power ratios of all frequency bands over time with the temporal development of CRS-R score.

of the spectral exponent was mainly present in the anterior and central brain regions (see Fig. 4D). Furthermore, a sleep episode occurred during Session 3, corresponding to a steepening of the slope and a drop in peak magnitude, as well as increased posterior dominance of theta power; however, this did not translate into meaningful changes in behavioral responsiveness compared to concurrent sessions.

In relation to the MFP and "ABCD" frameworks, both classifications were consistent and aligned across sessions. Sessions 1 and 3 showed peaks in both the theta and alpha bandwidths, corresponding to Type III and "non-ABCD" profiles. Sessions 2–6 were characterized by a single peak in the theta bandwidth, corresponding to Type II and Type "B" profiles. Finally, Session 7 was classified as a Type I and Type "A" profile, with the absence of a peak in the 1–14 Hz (see Fig. 6, Supplementary Fig. S8 for all PSD plots used to classify).

To provide clinical context, scores changed from GOSE 4/DRS 12/FIM 70 at 3 months, to GOSE 4/DRS 11/FIM 60 at 6 months, and to GOSE 4/DRS 8/FIM 90 at 12 months (see Supplementary Fig. S10).

Discussion

This case series is the first to characterize longitudinal changes in EEG spectral features in individuals with an acute-to-subacute DoC following sTBI. We tracked daily transitions across different states of consciousness using repeated CRS-R assessment in a sample that was as homogeneous as possible in terms of sex, age, etiology, and DAI severity.

Cases 1 and 2 displayed trajectories of good behavioral recovery of consciousness, as they transitioned across at least three states of consciousness (i.e. UWS, MCS−, MCS+, eMCS) and reached a diagnosis of eMCS by the end of the study protocol. In contrast, Cases 3 and 4 illustrate cases of an unfavorable behavioral recovery trajectory. Both participants remained stable and showed only marginal improvements of CRS-R score over the testing period,

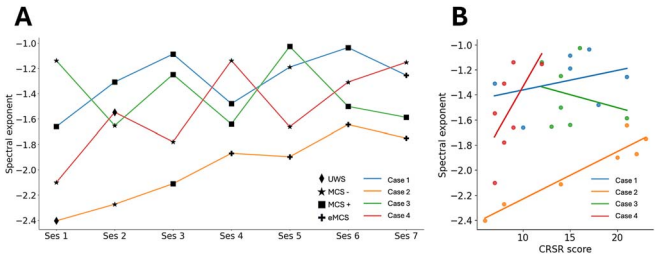

Figure 5. (A) Spectral exponent progression over time for all cases (B) Correlation between the spectral exponent and the CRS-R score for all cases for visualization purposes only.

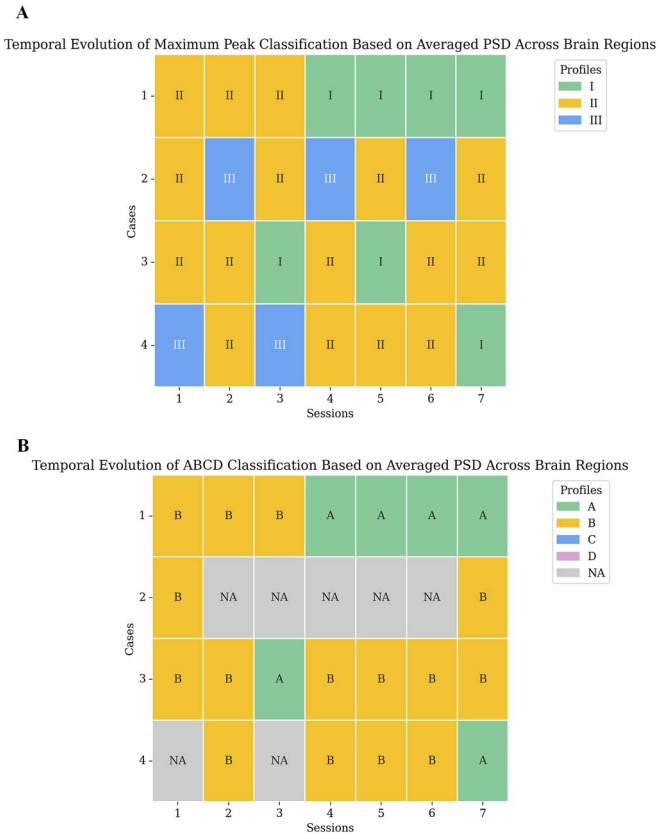

Figure 6. (A) Temporal evolution of maximum peak classification based on averaged PSD across brain regions and hemispheres (B) Temporal evolution of "ABCD" classification based on averaged PSD across brain regions and hemispheres.

with diagnoses shifting between MCS− and MCS+ states. The longitudinal analysis of daily EEG recordings revealed important variations in the analyzed features: (1) the aperiodic component, (2) the power spectral, (3) the spatial power gradients, (4) MFP, and (5) the ABCD frameworks both within the similar diagnostic categories and across participants.

The aperiodic component

Cases 1 and 2 showed improvements in behavioral responsiveness and exhibited a gradual flattening of the EEG spectral slope. In Case 2, the progressive flattening of the spectral exponent across sessions nearly paralleled the gradual behavioral improvement measured by the CRS-R, suggesting its association with the level of behavioral responsiveness. These results align with previous studies showing that the flattening of the spectral exponent indexes recovery from pharmacological and pathological unconsciousness (Colombo et al. 2019, Maschke et al. 2023) and stroke (Lanzone et al. 2022).

The correlation between the spectral exponent and level of consciousness was less consistent for Cases 3 and 4 who showed only marginal improvements of CRS-R scores across sessions. Despite relatively stable responsiveness, the spectral slope showed large fluctuations over time (Case 3) or a strong flattening of the spectral slope (Case 4). This discrepancy raises the possibility that changes in levels of consciousness could be captured on a neurophysiological level but not reflected behaviorally.

This case series suggests that while behavioral improvements in responsiveness after sTBI may correspond with a flattening of the spectral slope—reflecting a shift from slow-wave dominance toward higher-frequency activity, this relationship is not consistent across all cases, indicating that neurophysiological changes may occur independently of behavioral progress and highlighting the complementary role of EEG markers in assessing recovery. Further research is needed to investigate the clinical value of the spectral slope flattening in the absence of behavioral improvements.

Spectral power and spatial gradients

In Cases 1 and 2, a decrease in the absolute power in theta and alpha frequency bands, paired with an increase in beta spectral power, was observed as patients progressed toward emergence from MCS. Both cases displayed increasing posterior dominance of alpha power and anterior dominance of theta power as behavioral responsiveness improved.

Case 3 displayed some changes over time in the spatial distribution of delta, theta, beta, and gamma, which shifted from initial ratios of 1 (i.e. equal distribution across the brain) to posterior dominance. Alpha power distribution remained posterior dominant, similar to Cases 1 and 2. Case 4 showcased no major changes in the spatial distribution of any frequency band, mirroring the static behavioral scores of consciousness.

The posterior dominance of alpha power is valuable for indexing potential behavioral responsiveness. However, tracking changes in spatial dominance and power distribution across all frequency bands—or the absence of such changes over time—provide a more comprehensive indicator of improvements in behavioral responsiveness. The shift in power toward higher frequency bands as consciousness improves is accompanied by a flattening of the spectral slope. Both measures are interdependent, and it is essential to consider them collectively for a more accurate assessment.

Considering spectral power alone has limitations, as changes in absolute power within a bandwidth can be misinterpreted if not paired with the aperiodic component. Among other factors, alpha power may be attenuated by lesion topology that disrupts thalamo–cortical circuits, limiting the generation of posterior alpha rhythms (van Wijngaarden et al. 2016). Additionally, patients in this population are especially prone to fluctuations in arousal—particularly in the ICU—where episodes of microsleep or drowsiness can lead to more diffuse alpha distributions (Wang and Lin 2022). Changes in the slope can appear as fluctuations in frequency power (Donoghue et al. 2021). Therefore, using features that are corrected for the spectral slope—such as peak frequency—is more informative for the assessment of DoC patients.

Maximum peak frequency

The MFP framework from Drążyk et al. (2024) revealed discrepancies, especially for the Type I profile. Type I, associated with UWS with minimal behavioral signs of awareness, was frequently observed when the behavioral diagnosis indicated higher states of responsiveness such as MCS+ up to eMCS. One hypothesis that could explain these discrepancies is local sleep-like cortical bistability, which is a phenomenon that occurs following brain injury, where disrupted arousal drive and cortico-cortical disfacilitation cause some cortical regions to go into brief silent states that generate high delta activity characteristic of the Type I profile, while nearby networks remain sufficiently integral and active to compensate and support purposeful behavior responsiveness (Drążyk et al. 2024, Massimini et al. 2024). In contrast, Type II profile overall corresponded more accurately with behavioral assessments, as it was predominantly associated with MCS-level responsiveness. Finally, the presence of peaks in both theta and alpha frequency bands resulted in a Type III profile classification for Cases 2 and 4. While this profile is associated with increased brain dynamics, it did align with the reported interpretability challenges as a wide range of behavioral diagnosis were observed (e.g. MCS−, eMCS). Considering the high heterogeneity in brain dynamics between individuals and the altered brain activity in response to brain lesion, limiting the framework to only three profiles based on spectral power highlights the need for more integrative approaches to reliably index consciousness.

The ABCD model

The "B" profile was observed in all cases and was revealed as the most prevalent profile across patients and time, with peaks located in the theta bandwidth, reflecting severe deafferentation in the corticothalamic circuity (Edlow, Claassen, et al., 2021a; Schiff 2023). Consistent with the MFP results, Case 1 transitioned into an "A" profile over time, contradicting his exhibited improvements in behavioral responsiveness. Additionally, Cases 2 and 4 displayed "non-ABCD" profiles, mirroring Type III profile from the MFP framework, as peaks were present in both theta and alpha frequency bands without a clear peak in the beta frequency band. Although Cases 1 and 2 achieved eMCS, this progression in behavioral responsiveness was not reflected in spectral profiles, as neither case shifted toward "C" and "D" profiles. Repeated assessments allowed us to capture changes in the EEG spectrum profile, equally reflecting both the progression in behavioral responsiveness or the absence of improvements. This approach allowed to control for fluctuations in states of consciousness which sTBI patients are prone to Curley et al. (2022). However, limiting the framework to four spectral categories seems insufficiently comprehensive, as recurring heterogeneous and non-ABCD profiles were observed across sessions and participants, even when sex, age, etiology, and lesion severity were controlled, and behavioral diagnoses remained consistent.

Advantages of using longitudinal electroencephalography to uncover neurophysiological improvements

Longitudinal EEG assessments have the potential to track gradual neurophysiological improvements, which may precede the manifestation of behavioral improvements. The CRS-R score relies only on participant's behavior and their ability to both follow and respond to commands to evaluate states of consciousness, making it prone to errors. Factors such as language deficit or aphasia, sensory or motor impairments, pain, fatigue, medication, environment, or concurrent conditions can cause an underestimation of a patient's true level of consciousness. Therefore, pairing behavioral assessments with repeated EEG monitoring paradigms, as done in this study, is key to providing a more accurate and comprehensive assessment. Upon further investigation of larger sample sizes, this approach could reveal neurophysiological improvements despite unchanging levels of behavioral responsiveness.

In addition, this case series highlights the importance of considering the relative change of neurophysiological markers of consciousness, rather than only the absolute value. Despite the homogeneity of patients in this study, measurements of EEG indices differed across participants and diagnostic states of consciousness. As an example, in Cases 1 and 2 behavioral improvements clearly aligned with a flattening of the spectral exponent. However, while Case 1 progressed from value of −1.66 to a maximum of −1.04, Case 2 only reached a maximum of −1.66. Comparing a single time-point measurement between individuals can be misleading, as the value of one patient's unconscious state may align with another patient's most conscious state.

These observations highlight the importance of accounting for individual differences and that a one-size-fits-all approach may be misleading. While being associated with states of consciousness, features derived from the EEG power spectrum are also highly heterogeneous, even among healthy individuals

(Näpflin et al. 2007, Gschwandtner et al. 2021). Because each patient's EEG is inherently idiosyncratic and because individuals with the same diagnosis can recover at different rates, the most meaningful insight comes from the direction and magnitude of within-patient change over time. Therefore, coherent longitudinal trajectories of multimodal tracking, rather than single-point measures, provide the clearest signal of emerging consciousness. Demuru and Fraschini (2020) showed that strong subject-specific characteristics featured by the aperiodic component can be used as a proxy to fingerprint individuals, especially in resting-state eye-open conditions. These discriminative properties distinguish individuals more efficiently than relying on spectral power within traditionally defined frequency bands (Demuru and Fraschini 2020). Relying solely on group-level analyses and assuming common optimal values or ranges of spectral markers, with deviations showing reduced level of behavioral responsiveness, might yield misdiagnosis or overshadow individual improvements.

Identifying "the optimal resting-state spectral marker" is an unachievable aim, as deviations from this value will always be biased by patients' demographics and individual brain function, structure, integrity, particularly in highly heterogeneous brain pathologies such as sTBI. Greater insights into recovery of consciousness may rather reside in capturing relative changes over time. Instead, we propose that longitudinal assessments and within-subject design are key to the development of generalizable clinical markers.

Limitations

The results are to be interpreted considering several limitations. First, only male participants were included in this study. Further research is needed to identify and validate markers in female patients and to investigate potential sex-related differences. Second, this study only included four cases. Longitudinal assessments conducted on larger cohorts are necessary to validate markers of consciousness across the broader population. Third, as the different pathophysiology of DoC etiologies can manifest distinctly in the EEG signal and its derivatives, we focused on a single etiology. This facilitated the development of indices validated in acute-to-subacute DoC and improved their specificity. However, longitudinal validation of markers of consciousness is required across etiologies other than sTBI. Fourth, this study does not clarify if the measured neurophysiological markers reflect states of consciousness or the severity of brain injury. Because we lacked stimulus-reactivity paradigms, systematic sleep–wake monitoring, and evoked-potential recordings, we were unable to apply the qualitative Forgacs classification or incorporate the multimodal biomarkers recommended by recent European Academy of Neurology guidelines. Future prospective studies should embed these complementary measures so their additive value can be tested alongside the automated, resting-state EEG indices used here. Fifth, EEG features can be confounded by non-physiological artifacts, such as the amplifier, the type of reference, ambient noise, as well as physiological sources, such as eye movements (Gao et al. 2017, Issa and Juhasz 2019). Considering the lack of control in ICU settings, EEG recordings in acute-to-subacute brain-injured patients are susceptible to spurious signals, raising the concern for their reliability. Furthermore, as EEG assessments were conducted under standard clinical care conditions, medications like clonidine were used to manage dexmedetomidine withdrawal and reduce sympathetic hyperactivity. However, it can affect EEG patterns, as some studies have reported variable effects on delta power and slight increases in alpha power (Sinkin et al. 2021, Alshaya et al. 2023). In this study, Patient 3 did not receive clonidine, while the other patients did at constant levels, which may have contributed to the observed EEG differences. Despite these limitations, repeated within-subject measurements helped to better isolate genuine neurophysiological changes across sessions.

Conclusion

Tracking the temporal progression of sTBI DoC patients using EEG metrics such as spatial ratios, the aperiodic component, and the location of the maximal peak can provide added sensitivity for measuring consciousness above and beyond behavioral responsiveness. This provides insights into brain dynamics that are complementary to behavioral assessment, emphasizing the relevance of integrating longitudinal neurophysiological tracking to understand recovery patterns of consciousness more comprehensively.

Acknowledgments

The authors want to thank families and patients who accepted to participate in this study, as well as the hospital care team that allowed for this project to be conducted.

Author contributions

Beatrice P. De Koninck (Conceptualization, Data curation, Formal analysis, Investigation, Methodology, Project administration, Software, Validation, Visualization, Writing—original draft, Writing—review & editing [lead]), Charlotte Marschke (Conceptualization [supporting], Formal analysis [equal], Investigation [equal], Methodology [equal], Validation [equal], Visualization [equal], Writing—original draft [supporting]), Marie-Michèle Briand (Investigation, Project administration, Writing—review & editing [supporting]), Amélie Apinis-Dehaies (Data curation, Investigation, Project administration, Resources, Writing—review & editing [supporting]), Daphnee Brazeau (Data curation, Investigation, Methodology, Project administration, Writing—review & editing [supporting]), Rosalie Girard-Pepin (Formal analysis, Investigation, Methodology, Validation, Writing—review & editing [supporting]), Geraldine Martens (Investigation, Writing—review & editing [supporting]), Virginie Williams (Conceptualization, Data curation, Investigation, Project administration, Writing—review & editing [supporting]), Caroline Arbour (Conceptualization, Investigation, Resources, Writing—review & editing [supporting]), David Williamson (Conceptualization, Methodology, Writing—review & editing [supporting]), Catherine Duclos (Methodology, Validation, Writing—review & editing [supporting]), Francis Bernard (Conceptualization, Investigation, Methodology, Resources, Writing—review & editing [supporting]), Stefanie Blain-Moraes (Conceptualization, Formal analysis, Investigation, Methodology, Resources, Supervision, Validation, Writing—review & editing [lead]), Louis De Beaumont (Conceptualization, Funding acquisition, Investigation, Methodology, Resources, Supervision, Validation, Writing—review & editing [lead]).

Supplementary data

Supplementary data is available at *Neuroscience of Consciousness* online.

Conflict of interest

The authors declare that the research was conducted in the absence of any commercial relationships that could be construed as a potential conflict of interest.

Funding

This study is funded by the New Frontiers in Research fund (NFRFE2021–00886). Doctoral training scholarship to BPDK is provided by the Fonds de recherche du Québec-Santé (BF2-313707) and Chaire Fondation Caroline Durand en traumatologie aigue de l'Université de Montréal.

Data availability

To ensure data quality, a double data entry process was implemented for all measurements. The collected data were stored on an on-site secured network infrastructure with regular backups on a maintained, dedicated server. To ensure confidentiality, each participant was assigned a unique anonymized ID, and the corresponding file linking to their original information was encrypted and securely stored.

References

AbilityLab. *Coma Recovery Scale—Revised*. Chicago, IL: Shirley Ryan AbilityLab, 2020. https://www.sralab.org/rehabilitation-measures/coma-recovery-scale-revised

Alnagger N, Cardone P, Martial C *et al.* The current and future contribution of neuroimaging to the understanding of disorders of consciousness. *Presse Med* 2023;**52**:104163. https://doi.org/10.1016/j.lpm.2022.104163

Alshaya A, Aldhaeefi M, Alodhaiyan N *et al.* Clonidine safety and effectiveness in the management of suspected paroxysmal sympathetic hyperactivity post-traumatic brain injury: a retrospective cohort study. *Sci Prog* 2023;**106**:1–12. https://doi.org/10.1177/00368504231201298

Bodien YG, Allanson J, Cardone P *et al.* Cognitive motor dissociation in disorders of consciousness. *N Engl J Med* 2024;**391**:598–608. https://doi.org/10.1056/NEJMoa2400645

Bruno M-A, Vanhaudenhuyse A, Thibaut A *et al.* From unresponsive wakefulness to minimally conscious PLUS and functional locked-in syndromes: recent advances in our understanding of disorders of consciousness. *J Neurol* 2011;**258**:1373–84. https://doi.org/10.1007/s00415-011-6114-x

Casali AG, Gosseries O, Rosanova M *et al.* A theoretically based index of consciousness independent of sensory processing and behavior. *Sci Transl Med* 2013;**5**:198ra105-198ra105. https://doi.org/10.1126/scitranslmed.3006294

Cassol H, Aubinet C, Thibaut A *et al.* Diagnostic, pronostic et traitements des troubles de la conscience. *NPG Neurol Psychiat Gériatr* 2018;**18**:47–59. https://doi.org/10.1016/j.npg.2017.04.001

Chennu S, Finoia P, Kamau E *et al.* Spectral signatures of reorganised brain networks in disorders of consciousness. *PLoS Comput Biol* 2014;**10**:e1003887. https://doi.org/10.1371/journal.pcbi.1003887

Chennu S, Annen J, Wannez S *et al.* Brain networks predict metabolism, diagnosis and prognosis at the bedside in disorders of consciousness. *Brain J Neurol* 2017;**140**:2120–32. https://doi.org/10.1093/brain/awx163

Claassen J, Kondziella D, Alkhachroum A *et al.* Cognitive motor dissociation: gap analysis and future directions. *Neurocrit Care* 2023;**40**:81–98. https://doi.org/10.1007/s12028-023-01769-3

Colombo MA, Napolitani M, Boly M *et al.* The spectral exponent of the resting EEG indexes the presence of consciousness during unresponsiveness induced by propofol, xenon, and ketamine. *NeuroImage* 2019;**189**:631–44. https://doi.org/10.1016/j.neuroimage.2019.01.024

Colombo MA, Comanducci A, Casarotto S *et al.* Beyond alpha power: EEG spatial and spectral gradients robustly stratify disorders of consciousness. *Cereb Cortex* 2023;**33**:7193–210. https://doi.org/10.1093/cercor/bhad031

Curley WH, Bodien YG, Zhou DW *et al.* Electrophysiological correlates of thalamocortical function in acute severe traumatic brain injury. *Cortex* 2022;**152**:136–52. https://doi.org/10.1016/j.cortex.2022.04.007

De Koninck BP, Brazeau D, Deshaies AA *et al.* Modulation of brain activity in brain-injured patients with a disorder of consciousness in intensive care with repeated 10-Hz transcranial alternating current stimulation (tACS): a randomised controlled trial protocol. *BMJ Open* 2024;**14**:e078281. https://doi.org/10.1136/bmjopen-2023-078281

Demertzi A, Tagliazucchi E, Dehaene S *et al.* Human consciousness is supported by dynamic complex patterns of brain signal coordination. *Sci Adv* 2019;**5**:eaat7603. https://doi.org/10.1126/sciadv.aat7603

Demuru M, Fraschini M. EEG fingerprinting: subject-specific signature based on the aperiodic component of power spectrum. *Comput Biol Med* 2020;**120**:103748. https://doi.org/10.1016/j.compbiomed.2020.103748

MNE Developers. *MNE—MNE 0.21.2 Documentation* 2012, 2020. https://mne.tools/stable/index.html.

Donoghue T, Haller M, Peterson EJ *et al.* Parameterizing neural power spectra into periodic and aperiodic components. *Nat Neurosci* 2020;**23**:1655–65. https://doi.org/10.1038/s41593-020-00744-x

Donoghue T, Schaworonkow N, Voytek B. Methodological considerations for studying neural oscillations. *Eur J Neurosci* 2021;**55**:3502–27. https://doi.org/10.1111/ejn.15361

Drążyk D, Przewrocki K, Górska-Klimowska U *et al.* Distinct spectral profiles of awake resting EEG in disorders of consciousness: the role of frequency and topography of oscillations. *Brain Topogr* 2024;**37**:138–51. https://doi.org/10.1007/s10548-023-01024-0

Edlow BL, Chatelle C, Spencer CA *et al.* Early detection of consciousness in patients with acute severe traumatic brain injury. *Brain J Neurol* 2017;**140**:2399–414. https://doi.org/10.1093/brain/awx176

Edlow BL, Sanz LRD, Polizzotto L *et al.* Therapies to restore consciousness in patients with severe brain injuries: a gap analysis and future directions. *Neurocrit Care* 2021;**35**:68–85. https://doi.org/10.1007/s12028-021-01227-y

Edlow BL, Claassen J, Schiff ND *et al.* Recovery from disorders of consciousness: mechanisms, prognosis and emerging therapies. *Nat Rev Neurol* 2021a;**17**:135–56. https://doi.org/10.1038/s41582-020-00428-x

Engemann DA, Raimondo F, King J-R *et al.* Robust EEG-based cross-site and cross-protocol classification of states of consciousness. *Brain J Neurol* 2018;**141**:3179–92. https://doi.org/10.1093/brain/awy251

Fins JJ. Disorders of consciousness, past, present, and future. *Camb Q Healthc Ethics* 2019;**28**:603–15. https://doi.org/10.1017/S0963180119000719

Forgacs PB, Frey H, Velazquez A *et al.* Dynamic regimes of neocortical activity linked to corticothalamic integrity correlate with outcomes in acute anoxic brain injury after cardiac arrest. *Annals of Clinical and Translational Neurology* 2017;**4**:119–29. Portico. https://doi.org/10.1002/acn3.385

Frohlich J, Chiang JN, Mediano PAM *et al.* Neural complexity is a common denominator of human consciousness across diverse regimes of cortical dynamics. *Commun Biol* 2022;**5**:1374–17. https://doi.org/10.1038/s42003-022-04331-7

Gao R, Peterson EJ, Voytek B. Inferring synaptic excitation/inhibition balance from field potentials. *NeuroImage* 2017;**158**:70–8. https://doi.org/10.1016/j.neuroimage.2017.06.078

Gentry LR. Imaging of closed head injury. *Radiology* 1994;**191**:1–17. https://doi.org/10.1148/radiology.191.1.8134551

Gerster M, Waterstraat G, Litvak V *et al.* Separating Neural Oscillations from Aperiodic 1/f Activity: Challenges and Recommendations. *Neuroinformatics* 2022;**20**:991–1012. https://doi.org/10.1007/s12021-022-09581-8

Giacino JT, Ashwal S, Childs N *et al.* The minimally conscious state: definition and diagnostic criteria. *Neurology* 2002;**58**:349–53. https://doi.org/10.1212/wnl.58.3.349

Giacino JT, Kalmar K, Whyte J. The JFK coma recovery scale-revised: measurement characteristics and diagnostic utility11No commercial party having a direct financial interest in the results of the research supporting this article has or will confer a benefit upon the authors or upon any organization with which the authors are associated. *Arch Phys Med Rehabil* 2004;**85**:2020–9. https://doi.org/10.1016/j.apmr.2004.02.033

Giacino, J. T., Schnakers, C., Rodriguez-Moreno, D., *et al.* (2009). Behavioral assessment in patients with disorders of consciousness: gold standard or fool's gold? In S. Laureys, N. D. Schiff, & A. M. Owen (Eds.), *Progress in Brain Research* (Vol. **177**, pp. 33–48). Amsterdam, Netherlands: Elsevier. https://doi.org/10.1016/S0079-6123(09)17704-X

Giacino JT, Fins JJ, Laureys S *et al.* Disorders of consciousness after acquired brain injury: the state of the science. *Nat Rev Neurol* 2014;**10**:99–114. https://doi.org/10.1038/nrneurol.2013.279

Giacino JT, Katz DI, Schiff ND *et al.* Practice guideline update recommendations summary: disorders of consciousness: report of the guideline development, dissemination, and implementation Subcommittee of the American Academy of neurology; the American congress of rehabilitation medicine; and the National Institute on Disability, Independent Living, and Rehabilitation Research. *Neurology* 2018;**91**:450–60. https://doi.org/10.1212/WNL.0000000000005926

Gibson RM, Chennu S, Owen AM *et al.* Complexity and familiarity enhance single-trial detectability of imagined movements with electroencephalography. *Clin Neurophysiol* 2014;**125**:1556–67. https://doi.org/10.1016/j.clinph.2013.11.034

Gosseries O, Zasler ND, Laureys S. Recent advances in disorders of consciousness: focus on the diagnosis. *Brain Inj* 2014;**28**:1141–50. https://doi.org/10.3109/02699052.2014.920522

Gramfort A, Luessi M, Larson E *et al.* MEG and EEG data analysis with MNE-python. *Front Neurosci* 2013;**7**:1–13. https://doi.org/10.3389/fnins.2013.00267

Gschwandtner U, Bogaarts G, Chaturvedi M *et al.* Dynamic functional connectivity of EEG: from identifying fingerprints to gender differences to a general blueprint for the Brain's functional organization. *Front Neurosci* 2021;**15**:683633. https://doi.org/10.3389/fnins.2021.683633

Issa MF, Juhasz Z. Improved EOG Artifact Removal Using Wavelet Enhanced Independent Component Analysis. *Brain Sciences* 2019;**9**:355. https://doi.org/10.3390/brainsci9120355

Jöhr J, Halimi F, Pasquier J *et al.* Recovery in cognitive motor dissociation after severe brain injury: a cohort study. *PLoS ONE* 2020;**15**:e0228474. https://doi.org/10.1371/journal.pone.0228474

Jordan KG. Neurophysiologic monitoring in the neuroscience intensive care unit. *Neurol Clin* 1995;**13**:579–626. https://doi.org/10.1016/S0733-8619(18)30035-5

King J-R, Sitt JD, Faugeras F *et al.* Information sharing in the brain indexes consciousness in noncommunicative patients. *Curr Biol* 2013;**23**:1914–9. https://doi.org/10.1016/j.cub.2013.07.075

Kondziella D, Friberg CK, Frokjaer VG *et al.* Preserved consciousness in vegetative and minimal conscious states: systematic review and meta-analysis. *J Neurol Neurosurg Psychiatry* 2016;**87**:485–92. https://doi.org/10.1136/jnnp-2015-310958

Lanzone J, Colombo MA, Sarasso S *et al.* EEG spectral exponent as a synthetic index for the longitudinal assessment of stroke recovery. *Clin Neurophysiol* 2022;**137**:92–101. https://doi.org/10.1016/j.clinph.2022.02.022

Laureys S, Owen AM, Schiff ND. Brain function in coma, vegetative state, and related disorders. *Lancet Neurol* 2004;**3**:537–46. https://doi.org/10.1016/S1474-4422(04)00852-X

Lehembre R, Bruno M-A, Vanhaudenhuyse A *et al.* Resting-state EEG study of comatose patients: a connectivity and frequency analysis to find differences between vegetative and minimally conscious states. *Funct Neurol* 2012;**27**:41–7.

Lendner JD, Helfrich RF, Mander BA *et al.* An electrophysiological marker of arousal level in humans. *eLife* 2020;**9**:e55092. https://doi.org/10.7554/eLife.55092

Liu Y, Zeng W, Pan N *et al.* EEG complexity correlates with residual consciousness level of disorders of consciousness. *BMC Neurol* 2023;**23**:140. https://doi.org/10.1186/s12883-023-03167-w

Marino MH, Whyte J. Treatment trials in disorders of consciousness: challenges and future directions. *Brain Sci* 2022;**12**:569. https://doi.org/10.3390/brainsci12050569

Maschke C, Duclos C, Owen AM *et al.* Aperiodic brain activity and response to anesthesia vary in disorders of consciousness. *NeuroImage* 2023;**275**:120154. https://doi.org/10.1016/j.neuroimage.2023.120154

Maschke C, Belloli L, Manasova D *et al.* The role of etiology in the identification of clinical markers of consciousness: comparing EEG alpha power, complexity, and spectral exponent (p. 2024.03.20.24304639). medRxiv. 2024. https://doi.org/10.1101/2024.03.20.24304639

Massimini M, Corbetta M, Sanchez-Vives MV *et al.* Sleep-like cortical dynamics during wakefulness and their network effects following brain injury. *Nat Commun* 2024;**15**:7207–15. https://doi.org/10.1038/s41467-024-51586-1

Näpflin M, Wildi M, Sarnthein J. Test–retest reliability of resting EEG spectra validates a statistical signature of persons. *Clin Neurophysiol* 2007;**118**:2519–24. https://doi.org/10.1016/j.clinph.2007.07.022

Piarulli A, Bergamasco M, Thibaut A *et al.* EEG ultradian rhythmicity differences in disorders of consciousness during wakefulness. *J Neurol* 2016;**263**:1746–60. https://doi.org/10.1007/s00415-016-8196-y

Rosanova M, Gosseries O, Casarotto S *et al.* Recovery of cortical effective connectivity and recovery of consciousness in vegetative patients. *Brain* 2012;**135**:1308–20. https://doi.org/10.1093/brain/awr340

Schiff ND. Cognitive motor dissociation following severe brain injuries. *JAMA Neurol* 2015;**72**:1413–5. https://doi.org/10.1001/jamaneurol.2015.2899

Schiff, N. D. (2016). Mesocircuit mechanisms underlying recovery of consciousness following severe brain injuries: model and predictions. In M. M. Monti & W. G. Sannita (Eds.), *Brain Function and Responsiveness in Disorders of Consciousness* (pp. 195–204). Cham, Switzerland: Springer International Publishing. https://doi.org/10.1007/978-3-319-21425-2_15

Schiff ND. Mesocircuit mechanisms in the diagnosis and treatment of disorders of consciousness. *Presse Med* 2023;**52**:104161. https://doi.org/10.1016/j.lpm.2022.104161

Schnakers C, Vanhaudenhuyse A, Giacino J *et al.* Diagnostic accuracy of the vegetative and minimally conscious state: clinical consensus versus standardized neurobehavioral assessment. *BMC Neurol* 2009;**9**:35. https://doi.org/10.1186/1471-2377-9-35

Seth AK, Bayne T. Theories of consciousness. *Nat Rev Neurosci* 2022;**23**:439–52. https://doi.org/10.1038/s41583-022-00587-4

Sinkin MV, Talypov A, Yakovlev A *et al.* Long-term EEG monitoring in patients with acute traumatic brain injury. *Z Nevrol Psikhiatr Im S S Korsakova* 2021;**121**:62–7. https://doi.org/10.17116/JNEVRO202112105162

Sitt JD, King J-R, El Karoui I *et al.* Large scale screening of neural signatures of consciousness in patients in a vegetative or minimally conscious state. *Brain* 2014;**137**:2258–70. https://doi.org/10.1093/brain/awu141

Stender J, Gosseries O, Bruno M-A *et al.* Diagnostic precision of PET imaging and functional MRI in disorders of consciousness: a clinical validation study. *Lancet (London, England)* 2014;**384**:514–22. https://doi.org/10.1016/S0140-6736(14)60042-8

Teasdale G, Jennett B. Assessment of coma and impaired consciousness. A practical scale. *Lancet (London, England)* 1974;**304**:81–4. https://doi.org/10.1016/s0140-6736(74)91639-0

Thibaut A, Schiff N, Giacino J *et al.* Therapeutic interventions in patients with prolonged disorders of consciousness. *Lancet Neurol* 2019;**18**:600–14. https://doi.org/10.1016/S1474-4422(19)30031-6

Thibaut A, Bodien YG, Laureys S *et al.* Minimally conscious state "plus": diagnostic criteria and relation to functional recovery. *J Neurol* 2020;**267**:1245–54. https://doi.org/10.1007/s00415-019-09628-y

Toker D, Pappas I, Lendner JD *et al.* Consciousness is supported by near-critical slow cortical electrodynamics. *Proc Natl Acad Sci* 2022;**119**:e202e4455119. https://doi.org/10.1073/pnas.2024455119

Walter N, Hinterberger T. Determining states of consciousness in the electroencephalogram based on spectral, complexity, and criticality features. *Neurosci Consciousness* **2022**:niac008. https://doi.org/10.1093/nc/niac008

Wang, Y., & Lin, Y. (2022). *Patterns and Clinical Significance of Abnormal Sleep EEG* (pp. 141–58). Springer, Singapore. https://doi.org/10.1007/978-981-16-4493-1_5

Wannez S, Heine L, Thonnard M *et al.* The repetition of behavioral assessments in diagnosis of disorders of consciousness. *Ann Neurol* 2017;**81**:883–9. https://doi.org/10.1002/ana.24962

van Wijngaarden JBG, Zucca R, Finnigan S *et al.* The impact of cortical lesions on Thalamo-cortical network dynamics after acute ischaemic stroke: a combined experimental and theoretical study. *PLoS Comput Biol* 2016;**12**:e1005048. https://doi.org/10.1371/JOURNAL.PCBI.1005048

Wutzl B, Golaszewski SM, Leibnitz K *et al.* Narrative review: quantitative EEG in disorders of consciousness. *Brain Sci* 2021;**11**:697. https://doi.org/10.3390/brainsci11060697

Neuroscience of Consciousness, 2025, **2025(1)**, **2025**, niaf028
https://doi.org/10.1093/nc/niaf028
Research Article